Appl Biochem Biotechnol
DOI 10.1007/s12010-015-1623-1

Predictor–Response Analysis of Fiber Optic Enzymatic Biosensors Constructed with Nonmodified *E. coli* BL21 (DE3) pGELAF+ Sensing 1,2-Dichloroethane

Cory D. Jensen [1,2,3,5] · **Cord Müeller** [1,4]

Received: 28 January 2015 / Accepted: 6 April 2015

Abstract Biosensor technology can lack methods to iteratively validate system outputs (i.e., signals) concomitantly with the development of mathematical models. We evaluated a nonmodified fiber optic enzymatic biosensor (FOEB—*Escherichia coli* BL21 (DE3) pGELAF+) sensing dichloroethane with a predictor–response statistical form. The linear regression technique applied with MATLAB functions correlated FOEB parameters to sensing responses that could be used to identify system characteristics and interactions. A FOEB specific metric (i.e. normalized sensitivity) is shown to be significant as a mixed sensing correlation metric suggesting that similar development parameters could be related to engineering design paradigms for biosensor (or whole cell biosensor) systems.

Keywords Fiber optic enzymatic biosensor · pH optode · Whole-cell biosensors · Signal interactions · Predictor–response regression

Abbreviations

h	hypothesis test result
kstat	test statistic of Lilliefor's test
ks2stat	test statistic of the two-sample Kolmogorov–Smirnov test
critval	critical value of the test statistic for Lilliefor's test
p	test specific *p* value
W	sum of the Ansari–Bradley ranks for the sample

✉ Cory D. Jensen
cory.jensen@alumni.colostate.edu

[1] Chemical and Biological Engineering, Colorado State University, Ft. Collins, CO, USA

[2] College of Computer Science and Engineering, Colorado School of Mines, Golden, CO, USA

[3] Engineering Research Services LLC, Golden, CO, USA

[4] Covidien, North Haven, CT, USA

[5] Present address: Golden, CO, USA

Published online: 24 April 2015

W^*	approximate normal statistic for the Ansari–Bradley test
X_i	regressors
X_1	day of use after construction
X_2	immobilized matrix size
X_3	optode sensitivity
X_4	change of analyte concentration in the measurement environment
X_5	response time
β_i	regression coefficients
y_i	sensor observations
ε_i	random disturbance

Introduction

Rigorous mathematical forms have not been developed specifically for fiber optic enzymatic biosensors (FOEB), and generally, biosensors/whole-cell biosensors (WCB) lack in validation efforts to confirm critical sensing mechanisms. These realities contribute to the field of complex system signal analysis as a state of the art research topic interesting to the biosensor research community (A. Dean, personal communication). Table 1 illustrates additional research areas that make use of WCB, endeavors that could also benefit from gaining insight into complex systems interactions.

FOEB have been shown to be capable of sensitive measurements, have been validated upon comparison with traditional analytical methods [1, 4, 5, 16, 18], are an emerging technology, and type of fiber optic biosensor [22] with both advantageous and unfavorable characteristics [4].

FOEB signal traces follow a general trend (Fig. 1—*left hand side*). Jensen [8] reviews and proposes additional modeling approaches for FOEB while demonstrating that arbitrary models can be developed similar to traces observed in the laboratory setting (Fig. 2, [8]).

Fluorescence-based sensing techniques are common, yet they pose significant modeling and characterization challenges [10, 22]. Initially, in the case of WCB an integratable biocomponent is required [7]. Further examples include: Song et al. [21]

Table 1 Sampling of state of the art whole-cell biotechnology-sensor applications that could benefit from novel analysis and engineering approaches

Topic	Relationship to FOEB	Source
Bioluminescient sensors	Long-term cell viability, biocatalysis, and instrumentation	Michelini et al. [12]
Field deployable microfluidic sensors	Sensor material and geometry response–performance dependencies	Bridle [3]
Genetically engineering in complex lab on a chip designs	Relationships to bioengineering and system performance	Roda et al. [19]
Configuration and instrumentation	Illustrates design variability	Bidmanova et al. [2]
Cell-coating encapsulation	Biocatalysis; tuning metabolic activity to the application	Park et al. [13]

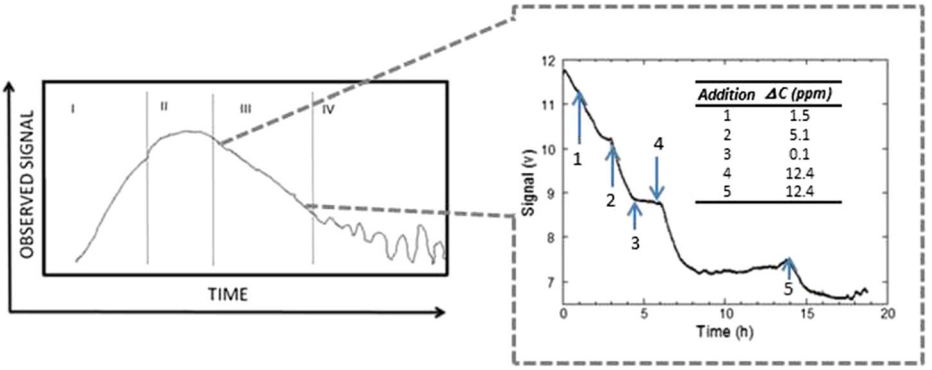

Fig. 1 *Left* Generalized nonmodified FOEB signal time course: (*I*) initial period of signal rise, (*II*) signal inflection, (*III*) period of constant decreasing signal, and (*IV*) erratic or not detectable signal. Note: This segmented pattern trace is not a scale and represents general trends from multiple FOEB used in the laboratory and in the field. *Right* Actual time course (i.e., signal trace) of *E. coli* BL21 (DE3) pGELAF+, photomultiplier tube setting of 700, FOEB sensitivity of 25.6, tested on the second day after construction, sensing DCA: volts (V) vs. time (h). Instrument signal is saved every 2 s into a data file; all data was graphed. Additions are noted by *arrows* and are summarized in the table as concentration changes (ppm) in the measurement environment

identified the significance of quenching mechanisms as related to polymer chemistry, and Fritzsche et al. [6] have shown variable absorbance characteristics are a function of fluorophore concentration when using a fluorescent dye similar to this research. Reardon et al. [16, 18] have reviewed photoluminescence-based biosensor technology specific to environmental applications, and early research by Reardon et al. [17] and Reardon and Bailey [15] reinforced the importance of identifying the metabolic state of cells during immobilization. Building on methods to support concerted and sustained biocatalysis immobilization has been a focus [11]. Additional study has characterized optoelectronic instrument operational parameters such as excitation optical power [14].

This research describes the use of pH optode-based FOEB with immobilized *Escherichia coli* BL21 (DE3) pGELAF+ [20] used to sense 1,2-dichloroethane (DCA). An optode is a sensing component that makes use of a chemical transducer, and the inclusion of cells constitutes a biosensor. Campbell et al. [4] recount the individual FOEB system components.

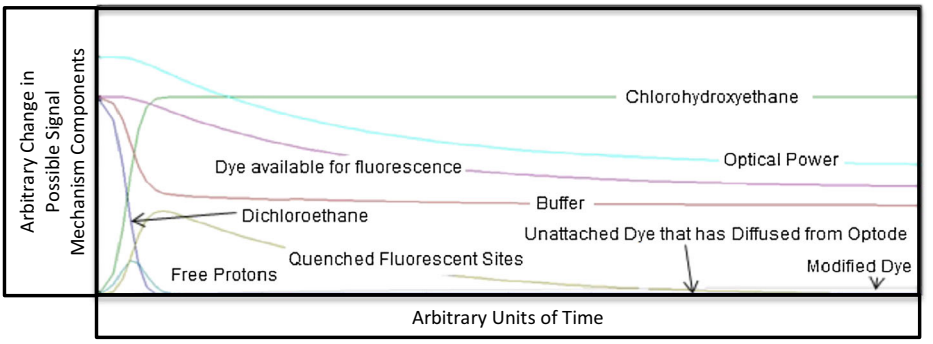

Fig. 2 Arbitrary FOEB signal traces similar to laboratory observations could be due to unconfirmed sensing components represented in differential form vs. time [8]. Optical power is the output that is displayed on an FOEB instrument

It was proposed that a full linear regression predictor–response model form, represented by Eqs. 1 and 2:

$$y = \beta X + \varepsilon \tag{1}$$

$$\varepsilon = N\left(O, \sigma^2 I\right) \tag{2}$$

can be used to characterize and benchmark performance of FOEB, where y is a column vector of observations, β is a vector of regression (i.e., correlation) coefficients, X is the matrix of regressors, and ε represents a vector of random disturbances (Table 2).

Materials and Methods

Microorganisms and Culture Conditions

E. coli BL21 (DE3) pGELAF+ [20] and *E. coli* Dh5α (Fisher Scientific) were grown at 30 °C with shaking in on quarter strength Luria–Bertani medium containing 100 μg ampicillin/mL. Harvested cells were stored in 10 mL of 20 mM phosphate-buffered saline solution (pH=7.4). *E. coli* Dh5α was utilized as a negative control.

Preparation of pH Sensitive Fluorescent Dye

The fluorochrome component–fluoresceinamine isomer I (Sigma-Aldrich) was used as described by Campbell et al. [4] using polyvinyl vinyl alcohol (Mallinckrodt Baker, Inc.) with a relatively low molecular weight (i.e., ~3,500) as the polymeric dye backbone. Air-dried solid dye material was weighed and made up to 5 % by weight with distilled water.

pH Optode Preparation

Five microliters of glutaraldehyde (Sigma-Aldrich), 25 μL fluorescent dye, and 5 μL of 6 M HCl were combined to chemically link the dye to the distal surface of a polished polymethylmethacrylate fiber optic lead, with optics of 0.5 μm diameter, 0.25 μm thick sheath, and a straight tip bayonet connector.

Table 2 List of parameters and levels considered in linear regressions

Parameters (levels)
X_1—Day of use after construction (1,2,3)
X_2—Matrix size (0.5 and 6 μL)
X_3—Sensitivity (specific to optode)
X_4—Concentration (ppm)
X_5—Response time (h)

Optode Storage Solution

Dried optodes were stored in pH 7.4 and 0.1 M Na_2HPO_4 phosphate-buffered saline (PBS) at room temperature prior to FOEB construction.

pH Optode Sensitivity Solutions

Sensitivity characterization solutions were made by mixing two buffered phosphate solutions. KH_2PO_4 (0.2 M) and 0.2 M K_2HPO_4 having pHs; 7.13 and 6.93. optode sensitivity is determined by calculating Δvolts divided by ΔpH (i.e., 0.20) upon obtaining a steady state signal when optodes are placed in their respective pH solutions (optodes with sensitivities at 20 or greater were used for FOEB construction).

Biosensor Construction

Alginic acid sodium salt (0.2 g) from (Sigma-Aldrich, St. Louis MO, USA) was dissolved in 5.0 mL of distilled water. Alginate solution was added in a 0.1:1 weight ratio of dry cells to alginate solution. Two volumes (i.e., 0.5 and 6 μL) of cell paste were pipetted to cover the fluorescent dye layer of an optode (Fig. 4). Optodes with cell paste were ionotropically gelled in 0.47 M $CaCl_2$ in an ice bath for 30 min. FOEB were then stored in buffered measurement solution (BMS) made of 1 mM pH 7.3 Tris buffer (Fisher Scientific), 0.15 M NaCl, and 0.025 M $CaCl_2$ at 4 °C prior to use.

Measurement Protocol

Measurements were performed in BMS at room temperature by adding known volumes of standard BMS DCA solutions. After DCA addition, a response was allowed to develop by observing voltage displayed via MadgeTech 2.0 software (MadgeTech) over time (Fig. 1), after Campbell et al. [4].

Optoelectronic Instrumentation

The optoelectronic instrument (i.e. Verstärker I) system was the same as previously used by Campbell et al. [4] and Das and Reardon [5].

FOEB Measurement Apparatus

A modification was made to the measurement vial method—a metal stabilizer with sample inlet and outlet ports was incorporated to secure FOEB during measurements and to maintain a constant measurement liquid volume [8].

Regression Analysis

Seven refined predictor–response forms were obtained (Table 3) from the full model that considered individual predictors, two-way and three-way interactions with the MATLAB 7.8.0.347 (R2009a) function: stepwise (the full model contains 25 terms). Stepwise provides a graphical user interface for user directed regression analysis or automatic regression analysis. The MATLAB Statistics toolbox functions; histfit, Ansari–Bradley, kstest2, Lilliefor's test, and

Table 3 Regression model number, description, and stepwise "Goodness-of-fit" statistics

Model	Model description	R^2	Ajd. R^2	RMSE	F	Intrcpt.	p value	Terms	Norm R^2
1	Full model	0.9267	0.7278	0.6188	4.6586	0	0.02	All terms	1.00
2	Single parameters with time	0.2694	0.0955	1.2178	1.5491	−1.0191	0.22	$\times_1$, $\times_2$, $\times_3$, $\times_4$, and $\times_5$	0.29
3	Single parameters without time	0.2663	0.1328	1.1043	1.9957	−1.1449	0.13	$\times_1$, $\times_2$, $\times_3$, and $\times_4$	0.29
4	Stepwise-selected model	0.5114	0.4477	0.8814	8.0251	−0.3596	0.0008	$\times_{13}$, $\times_{23}$, and $\times_9$	0.55
5	Time dep., directed	0.6139	0.5636	0.7835	12.19	−0.3953	6.00E-05	$\times_5$, $\times_{19}$, and $\times_{25}$	0.66
6	Time indep., directed	0.5448	0.4364	0.8904	5.026	−4.908	0.0003	$\times_1$, $\times_2$, $\times_6$, $\times_8$, and $\times_{22}$	0.59
7	Hybrid directed	0.6489	0.5435	0.8012	6.1601	0.6312	0.0009	$\times_3$, $\times_5$, $\times_7$, $\times_9$, $\times_{13}$, and $\times_{15}$	0.70
8	With norm. sens.	0.7694	0.7145	0.6337	14.015	−0.79	4.33E-6	$\times_5$, $\times_{10}$, $\times_{19}$, $\times_{25}$, norm. sens.	0.83

Reduced form regressors are included as Terms. R^2 values are normalized to the over fit model no. 1

plotmatrix were used to characterize regressed models (Table 5). The sum of square errors and degree of freedom for each regressed model were also calculated (Table 5).

Results and Discussion

Nonmodified FOEB Responses

Figure 1 (*left hand side*) is a general depiction of nonmodified FOEB signal over time. The dynamic nature of this signal can be challenging to interpret. The signal can be separated into four distinct regions: (I) an initial rise (where 520-nm-emission intensity increases linearly); (II) a transition phase where the signal trace undergoes inflection (i.e., maximum fluorescent excitation has occurred and a new dominant "anti-excitation emission" mechanism takes over, therefore, reducing the 520-nm-emission intensity); (III) a period of steadily declining signal that can be perturbed upon analyte addition to the system; and (IV) a period where either the signal reaches a minimum constant signal (i.e., out of the range of the instrument) or becomes erratic. An erratic and unpredictable signal has been shown to be the result of a failing photo multiplier tube, a failing excitation light source, or a fluorescent dye layer that is not static with respect to the distal optic surface. All analyte signals for this research were obtained during period III (e.g., Fig. 1—*right hand side*). All viable sensors were used for only one measurement period (n=27).

Statistical Predictor–Response Model

Previous investigation has shown that nonmodified *E. coli* BL21 (DE3) pGELAF+ FOEB lose biocatalytic activity within a span of nearly 3 days [9]; time-sensitive use of WCB is a common consideration (Table 1). Several "goodness-of-fit" statistics are displayed with the seven-reduced form models (Table 3).

Table 4 Regression model, description, and regressors with associated regression coefficients (and p value)

Model	Model name	Regressors variable correlation coefficient (p-value)					
4	Stepwise-selected	$\times_{13}$	$\times_{23}$	$\times_{9}$			
		0.0074 (0.0001)	−0.037 (0.004)	0.343 (0.03)			
5	Time, dep. directed	$\times_{5}$	$\times_{19}$	$\times_{25}$			
		0.4932 (0.0206)	0.0068 (0.0000)	−0.0569 (0.0001)			
6	Time indep., directed	$\times_{1}$	$\times_{2}$	$\times_{6}$	$\times_{8}$	$\times_{22}$	
		2.8943 (0.02)	5.2285 (0.013)	−2.6872 (0.012)	−0.1265 (0.015)	0.0054 (0.002)	
7	Hybrid	$\times_{3}$	$\times_{5}$	$\times_{7}$	$\times_{9}$	$\times_{13}$	$\times_{15}$
		−0.1149 (0.005)	2.0622 (0.0009)	0.06575 (0.0028)	−0.9374 (0.005)	0.0125 (0.001)	−0.0909 (0.002)
8	With norm. sens.	$\times_{5}$	$\times_{10}$	$\times_{19}$	$\times_{25}$	norm. sens.	
		0.7761 (0.003)	−0.0272 (0.02)	0.0099 (0.0000)	−0.0770 (0.000)	71.11 (0.0013)	

Table 4 summarizes details of the four regression forms with interacting terms; one that the stepwise is identified with recommended regression selection steps (Eq. 3—model 4), one that the user directed and considers response time dependence (Eq. 4—model 5), one that is a user-directed form that does not include response time dependence (Eq. 5—model 6), and a hybrid "best-fit" model (Eq. 6—model 7) that was also selected by the user. User directed means that the predictors were moved in and out of the regression analysis manually and that the stepwise algorithm was not used.

$$y = \beta_0 + \beta_9 x_1 x_5 + \beta_{13} x_3 x_5 + \beta_{23} x_1 x_4 x_5 + \varepsilon \tag{3}$$

$$y = \beta_0 + \beta_5 x_5 + \beta_{19} x_2 x_3 x_4 + \beta_{25} x_2 x_4 x_5 + \varepsilon \tag{4}$$

Table 5 Additional statistical analysis of regressed models 4–8

Statistical analysis	Test stat.	Regression model				
		4	5	6	7	8
Sum of square errors		18.8	22.6	20.1	24.0	27.8
Degrees of freedom		23	23	21	20	21
Ansari–Bradley test	p	0.7818	0.8626	0.2253	0.5562	0.5332
	W	370	373	343	395	396
	W*	−0.2769	−0.1731	−1.2126	0.5885	0.6231
Two-sample Kolmogorov–Smirnov test	p	0.4656	0.2793	0.4656	0.4656	0.4656
	ks2stat	0.2222	0.2593	0.2222	0.2222	0.2222
Lilliefor's test	p	0.3523	0.5	0.0074	0.5	0.5
	h	0	0	1	0	0
	kstat	0.1232	0.0677	0.1989	0.1013	0.0949
	critval	0.1669	0.1669	0.1669	0.1669	0.1669

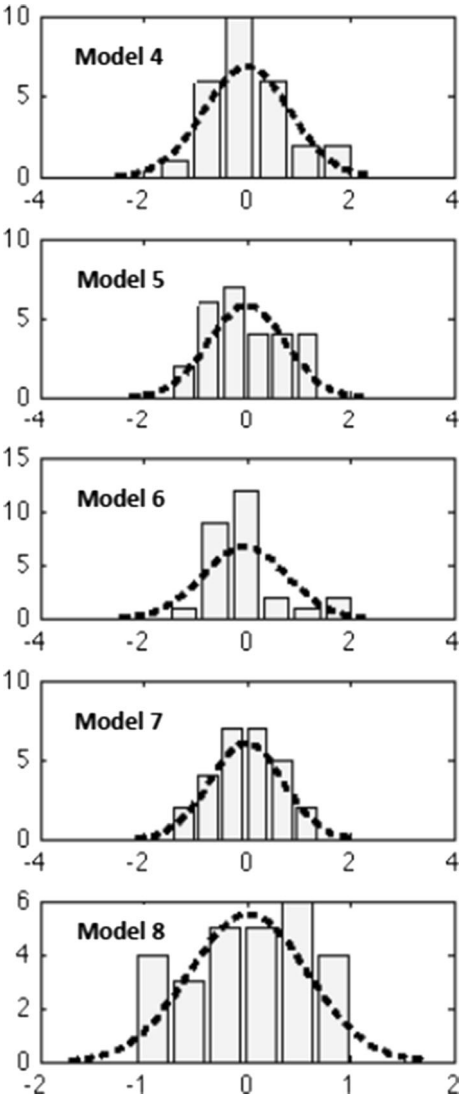

Fig. 3 Regressed models 4–8 residuals plotted with the MATLAB function—histfit

$$y = \beta_0 + \beta_1 x_1 + \beta_2 x_2 + \beta_6 x_1 x_2 + \beta_8 x_1 x_4 + \beta_{22} x_1 x_3 x_4 + \varepsilon \tag{5}$$

$$y = \beta_0 + \beta_3 x_3 + \beta_5 x_5 + \beta_7 x_1 x_3 + \beta_9 x_1 x_5 + \beta_{13} x_3 x_4 + \beta_{15} x_4 x_5 + \varepsilon \tag{6}$$

Of the base models that consider individual parameters and interacting terms (models 1–7); Table 4 shows that model 7 best explains observed data (R^2=0.6489); that model 5 best accounts for the inclusion of multiple terms (adj. R^2=0.5636) and explained variance (F= 12.19). Focusing on the interaction reduced forms, Table 4 also shows that highly significant

interactions were identified with predictors ($\times_{13}$—p value=0.0001, $\times_{19}$—p value<0.0001, and $\times_{25}$—p value<0.0000). These predictors represent the following interactions, respectively; (1) sensitivity-analyte concentration, (2) FOEB configuration-sensitivity-analyte concentration, and (3) FOEB configuration-analyte concentration-sensing response time.

Reduced models were also characterized with several MATLAB statistical toolbox analyses (Table 5) and Fig. 3 shows residual analysis results for Eqs. 3–6 and 8 (i.e., models 4–8). All reduced model forms were found to be representative of the same distribution from which they were derived (i.e., y_i) via the Ansari–Bradley and two-sample Kolmogorov–Smirnov tests. Residual analysis suggests that normalized fits are centered about zero (Fig. 3). Finally, Lilliefor's test indicates that model 6 results are not normal; this finding could have implications if a distribution of this model were to be used in future modeling simulations. However, initial results suggest that model 5 seems to be an outcome of this research that could be most likely to be used for future application.

For the time-independent analysis (i.e., model 6), the size of the immobilized matrix (X_2) has the largest positive regression coefficient when compared to all models. Physically, this suggests that diffusion effects could be implicated for the drastically different geometries (Fig. 4), possibly even unsuspecting reaction or absorption mechanisms indicating that further understanding of matrix, cell, and matrix–cell performance is required.

As a means to identify proper function of biocatalyst, a colorimetric pH sensitive agar plate method was devised to select for microorganism colonies that demonstrate a phenotype consistent with an ability to interact with the analyte of interest [8]. Additional methods to validate FOEB capability prior to use is desired, e.g., a test similar to a live-dead assay could be utilized in combination with parameters described in this research to better characterize WCB or modify them (e.g., [5, 11]).

These results suggest that bench top characteristics can be used to identify system interactions, suggests that further characterization can be required, and in both cases, can be used to direct the science-engineering of FOEB and WCB systems. It is also proposed that unique information (e.g., superior performance) can be identified. Specific to FOEB, we propose a normalized sensitivity metric. Normalized sensitivity is represented by Eq. 7 and is simply a

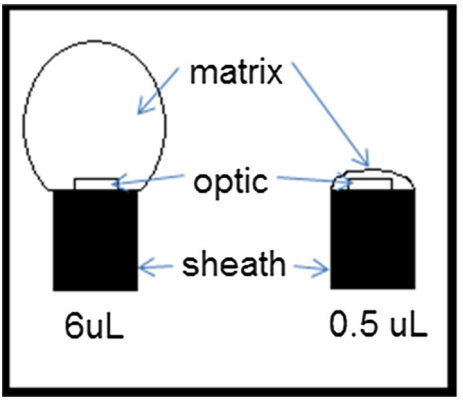

Fig. 4 Contrast of the appearance of FOEB used for this research: 6.0 (*left*) and 0.5 μL (*right*) of an immobilized whole-cell matrix

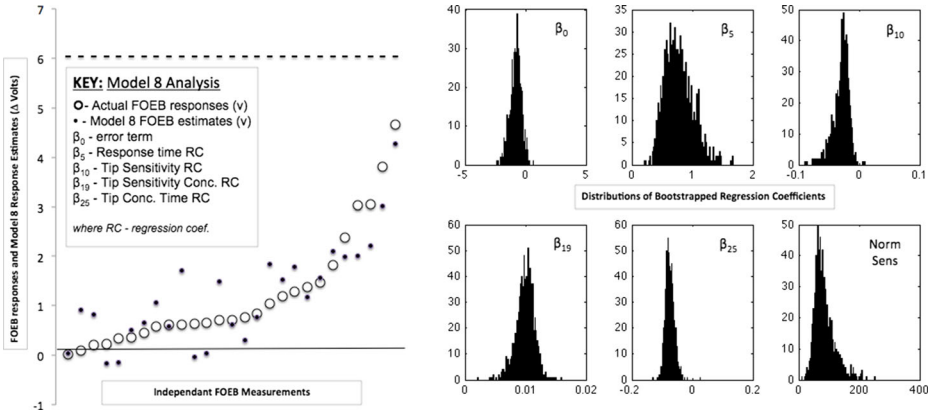

Fig. 5 *Left* Observed responses (*open circle*) graphed with model 8 estimates (*black dots*) for all observations; *dashed line* represents the upper 95 % confidence interval with averaged responses as model inputs. *Right* Histograms of a MATLAB algorithm used to determine bootstrapped regression coefficients for model 8 with 1,000 simulations; upper 95 % bootstrap values were used as correlation coefficients for *dashed line*

FOEB's optode sensitivity divided by sensing event's Δ voltage/Δ change of analyte concentration in the measurement environment.

$$Normalized\ Sensitivity = \frac{Optode\ Sensitivity}{\frac{Sensed\ \Delta\ V}{\Delta\ Analyte\ Conc}} \tag{7}$$

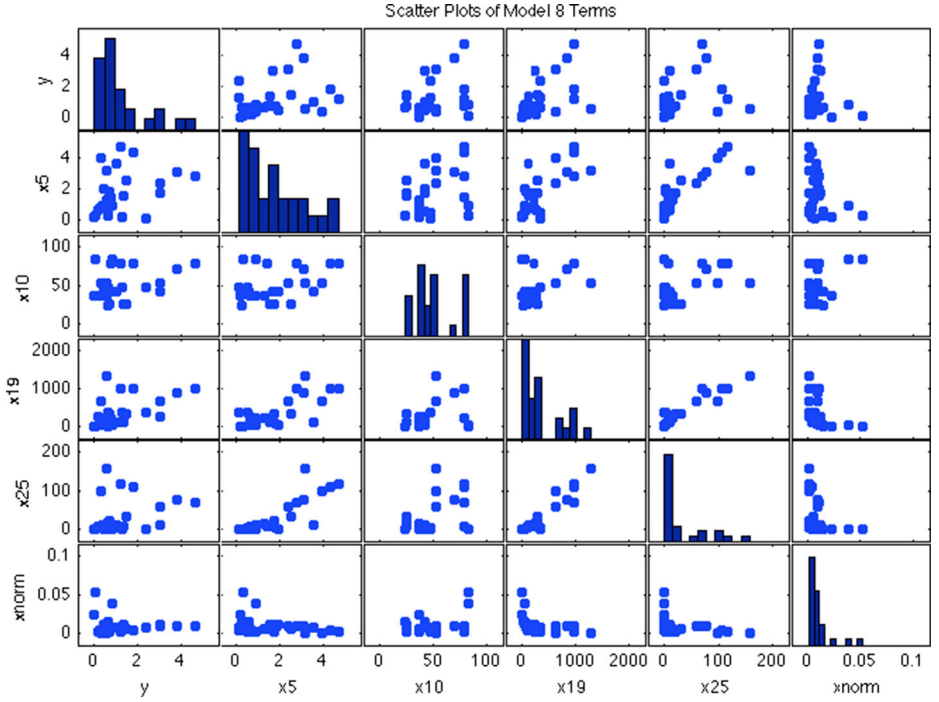

Fig. 6 Matrix plot of model 8 responses and variables

Equation 7 should be indicative not only of the optode's quality, but also of the entire FOEB systems performance. Normalized sensitivity was incorporated into a user directed regression and resulted in model 8 (Eq. 8).

$$y = \beta_0 + \beta_5 x_5 + \beta_{10} x_2 x_3 + \beta_{19} x_2 x_3 x_4 + \beta_{25} x_2 x_4 x_5 + \beta_{ns} norm\_sens + \varepsilon \quad (8)$$

As a result of incorporating the normalized sensitivity into an analysis, a new best performing model (with the trade-off of adding another predictor, i.e., $\times_{10}$) was identified with a R^2 value of 0.77. Moving the regressor $\times_{10}$ out of model 8 resulted in an R^2 value of 0.70. No additional mixed model metrics contributed to an R^2 value higher than obtained with model 8.

Overall, the selected benchmark parameters collected in experiments seem cable of explaining nearly 83 % of observed data (assuming the over-fit R^2 value of model 1 as an achievable limit). Actual FOEB responses are plotted with model 8 estimates and results from a MATLAB algorithm that determined distributions of bootstrapped regression coefficients for model 8 (Fig. 5).

Finally, the MATLAB function plotmatrix was used to compare model 8 parameters in scatterplots to better illustrate pair-wise interactions (Fig. 6).

Conclusions

It was concluded that predictor–response model that forms with correctly identified benchmark parameters could be developed to further guide the science-engineering and development of FOEB and WCB. It was also concluded that *E. coli* BL21 (DE3) pGELAF+ FOEBs can be applied to sense DCA in ppm to ppb concentrations. It was concluded that with significant sets of data, biotechnologists have tools available (e.g., MATLAB) to refine and validate results. Finally, it is proposed that appropriate WCB metrics could be used to better describe system performance.

Acknowledgments This research was made possible by ESTCP Project Number CU-0115, the Colorado State University, Dr. DB Janssen's laboratory (that developed *E. coli* BL21 (DE3) pGELAF+), the Colorado School of Mines, and Dr. Kenneth F. Reardon. Thanks to Dr. William Navidi for conversation on the topic of regression models. Special thanks to Brandon Cooksey who made and characterized several of the optodes used for this research. Thanks in particular not only to Dean and Professor Anthony Dean, Dr. David Muñoz, and Dr. Daniel Kaffine, but also to all of my colleagues for inspiring tenacious motivation.

References

1. Acha, V., Willis, W. B., Das, N., & Reardon, K. F. (2003). Fiber optic biosensors for halogenated organics in ground water. Proceedings of the 225th American Chemical Society National Meeting.
2. Bidmanova, S., Chaloupkova, R., Damborsky, J., & Prokop, Z. (2010). Development of an enzymatic fiber-optic biosensor for detection of halogenated hydrocarbons. *Analytical and Bioanalytical Chemistry, 398*, 1891–1898.
3. Bridle, H., Miller, B., & Desmulliez, M. P. (2014). Application of microfluidics in waterborne pathogen monitoring: a review. *Water Research, 55*, 256–271.
4. Campbell, D. W., Müeller, C., & Reardon, K. F. (2006). Development of a fiber optic enzymatic biosensor for 1,2-dichloroethane. *Biotechnology Letters, 28*, 883–887.
5. Das, N., & Reardon, K. F. (2012). Fiber-optic biosensor for the detection of atrazine: characterization and continuous measurements. *Analytical Letters, 45*, 251–261.
6. Fritzsche, M., Barreiroa, C. G., Hitzmanna, B., & Scheper, T. (2007). Optical pH sensing using spectral analysis. *Sensors and Actuators, B, 128*, 133–137.

7. Janssen, D. B., Scheper, A., Dijkhuizen, L., & Witholt, B. (1985). Degradation of halogenated aliphatic compounds. *Applied and Environmental Microbiology, 49*, 673–677.
8. Jensen, C. D. (2015). Emerging & applied environmental biotechnology: fiber optic biosensors and integrated macrophyte systems. Ph. D Dissertation. Fort Collins, Colorado State University.
9. Jensen, C. D., & Reardon, K. F. (2006). Effects of biosensor construction, storage time, and measurement environment on the performance of a dehalogenase based optoelectronic enzymatic biosensor. Poster Presentation—3rd Annual WEF/AWWA Student Conference at Colorado State University, Fort Collins CO, USA.
10. Lackowicz, J. R. (1999). *Principles of fluorescence spectroscopy* (2nd ed.). New York: Kluwer Academic Plenum Publisher.
11. Mateo, C., Palomo, J. M., Gloria Fernandez-Lorente, G., Guisan, J. M., & Fernandez-Lafuente, R. (2007). Improvement of enzyme activity, selectivity and stability via immobilization techniques. *Enzyme and Microbial Technology, 6*, 1451–1463.
12. Michelini, E., Cevenini, L., Calabretta, M. M., Spinozzi, S., Camborata, C., & Roda, A. (2013). Field-deployable whole-cell bioluminescent biosensors: so near and yet so far. *Analytical and Bioanalytical Chemistry, 405*(19), 6155–6163.
13. Park, J. H., Yang, S. H., Lee, J., Ko, E. H., Hong, D., & Choi, I. S. (2014). Nanocoating of single cells: from maintenance of cell viability to manipulation of cellular activities. *Advanced Materials, 26*(13), 2001–2010.
14. Pieper, S. B., Mestas, S., Lear, K. L., Zhong, X., & Reardon, K. F. (2008). Emission characteristics of ruthenium complex as optical transducer for phosphorescence biosensors. *Applied Physics Letters, 92*, 081915.
15. Reardon, K. F., & Bailey, J. E. (1992). Activity regeneration in continuous *Clostridium acetobutylicum* bioconversions of glucose. *Biotechnology Progress, 8*, 316–326.
16. Reardon, K. F., Campbell, D. W., & Müller, C. (2009). Optical fiber enzymatic biosensor for reagentless measurement of ethylene dibromide. *Engineering in Life Sciences, 9*, 291–297.
17. Reardon, K. F., Scherper, T., Anders, K. D., et al. (1990). Novel application of fluorescence sensors. *Applied Biochemistry and Biotechnology, 24*, 363–374.
18. Reardon, K. F., Zhong, Z., & Lear, K. L. (2009). Environmental applications of photoluminescence-based biosensors. *Advances in Biochemical Engineering/Biotechnology, 116*, 99–123.
19. Roda, A., Cevenini, L., Borg, S., Michelini, E., Calabretta, M. M., & Schüler, D. (2013). Bioengineered bioluminescent magnetotactic bacteria as a powerful tool for chip-based whole-cell biosensors. *Lab on a Chip, 13*(24), 4881–4889.
20. Schanstra, J. P., Rink, R., Pries, F., & Janssen, D. B. (1993). Construction of an expression and site-directed mutagenesis system of haloalkane dehalogenase in *Escherichia-coli. Protein Expression and Purification, 4*, 479–489.
21. Song, L. L., Hennink, E. J., Young, I. T., et al. (1995). Photobleaching kinetics of fluorescein in quantitative fluorescein fluorescence microscopy. *Biophysical Journal, 68*, 2588–2600.
22. Wang, X. D., & Wolfbeis, O. S. (2012). Fiber-optic chemical sensors and biosensors (2008–2012). *Analytical Chemistry, 85*(2), 487–508.